

Time domain measurement of spin-dependent recombination

Christoph Boehme^{a)} and Klaus Lips

Hahn-Meitner-Institut Berlin, Abteilung Silizium-Photovoltaik, Kekuléstr. 5, D-12489 Berlin, Germany

(Received 11 June 2001; accepted for publication 26 October 2001)

A defect characterization method is presented, the time domain measurement of spin-dependent recombination (TSR). Recombination between paramagnetic states is changed rapidly by electron spin resonant excitation through strong nanosecond microwave pulses. After the pulse, a slow relaxation of the recombination rate towards its steady state takes place. By measuring the current transient after the resonant pulse, information about dissociation and recombination probabilities of spin pairs is directly obtained for a distinct recombination path. Dangling bond recombination in microcrystalline silicon was used as model process for the demonstration of TSR. © 2001 American Institute of Physics. [DOI: 10.1063/1.1428623]

Spin-dependent recombination in semiconductors was first reported by Lepine.¹ He showed that the photoconductivity of silicon decreases when the paramagnetic defects are subjected to electron spin resonance (ESR). A model that could explain this observation was later developed by Kaplan, Solomon, and Mott² (KSM model) who introduced a picture of intermediate pair states of electrons and holes which exist for a certain time prior to recombination. As an example, such pairs form in disordered semiconductors when an electron is trapped in a band tail state in proximity to a neutral dangling bond.³ The effect of spin dependent recombination is used in electrically detected magnetic resonance (EDMR), a defect spectroscopy method which is able to characterize electronically active defects of semiconductors qualitatively and quantitatively with a sensitivity orders of magnitude better than ESR.³ Such investigations have been performed on various systems of semiconductor structures and devices in the past.³⁻⁹

While ESR and continuous wave (cw) EDMR both provide information about the type, density, and local structure of distinct defects, they fail to give quantitative information on how they actually interact electronically with charge carriers. Previous efforts to study the recombination dynamics were carried out by Eickelcamp *et al.*⁷ who described the lineshape dependence of cw-EDMR signals from recombination and dissociation probabilities. Hiromitsu *et al.*¹⁰ took a first approach to extract information about recombination dynamics from the time domain of cw EDMR by measuring the transients between the steady states of cw EDMR at phthalocyanine/C₆₀-heterojunctions. The drawback of these methods has always been the poor extractability of the wanted information from the given experimental data leading only to crude estimates of limits for the recombination and dissociation probabilities.

As long as coherent spin effects of the recombining charge carriers are negligible in comparison to incoherent effects such as recombination, dissociation, and spin relaxation, spin-dependent recombination in the KSM picture can accurately be described with rate equations. This rate equation model matches the much more complicated quantum

mechanical approach by statistical Liouville equations and is able to explain the nature of the experimental results presented below in an even more illustrative way.

We treat spin-dependent recombination according to the rate model illustrated in Fig. 1. The ensemble is represented by the number of given triplet states $n_T(t)$ and singlet states $n_S(t)$. The generation rate g of pairs is equal for each state and therefore three times as high for the three triplet states as for the singlet state. Dissociation is state independent and has the probability d while recombination with probability r can only take place out of singlet states. The mutual exchange probability w between singlet and triplet states represents influences by spin-lattice relaxation as well as the resonant microwave. Electron spin resonance takes place when a spin system which is exposed to a constant magnetic field B_0 is excited by a resonant electromagnetic wave with a frequency ω that matches the spins Larmor frequency according to the resonance condition $\hbar\omega = g\mu_B\mathbf{S}\cdot\mathbf{B}$. The right-hand side herein represents the energy split of the spin states due to the magnetic field interaction of the magnetic moment which is connected to the spin through the Bohr magneton μ_B and the Landé factor g . The intensity of the radiation in the resonance case is then connected to the exchange rate w with a square root dependence. The model given above leads directly to a simple inhomogeneous system of first order ordinary differential equations (ODE)

$$\partial_t \begin{pmatrix} n_T \\ n_S \end{pmatrix} = \begin{pmatrix} -[d+w] & w \\ w & -[d+r+w] \end{pmatrix} \begin{pmatrix} n_T \\ n_S \end{pmatrix} + \frac{g}{4} \begin{pmatrix} 3 \\ 1 \end{pmatrix}, \quad (1)$$

whose solutions can be found by an addition of the steady

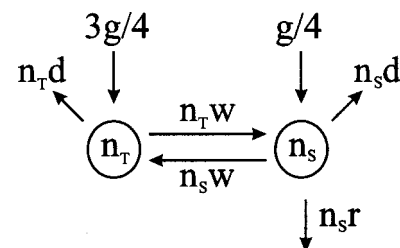


FIG. 1. Sketch of the rate model of KSM-pair recombination. Pair dissociation can take place from any state while recombination is possible from states with singlet content only.

^{a)}Electronic mail: boehme@hmi.de

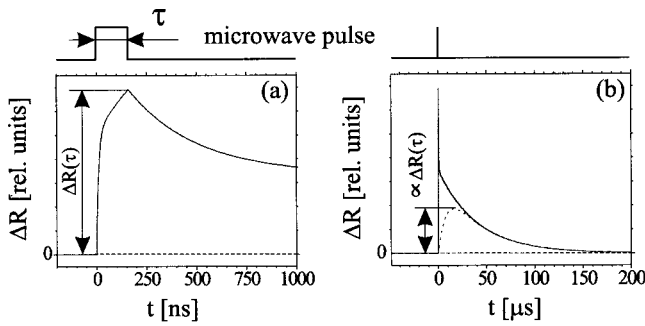


FIG. 2. Calculation of the recombination change according to the model predictions. (a) The double exponential increase during the pulse of length τ depends on the spin flip probability w and the recombination probability r . Under the given conditions, the initial exponential decay of ΔR after the pulse is determined only by r . (b) The solid line represents the transient of Fig. 2(a) on a 200 times extended time scale. Note that a second decay with a clearly longer time constant is present. The dotted line is a simulation of the transient tanking the time constant of real current amplifiers into account.

state solution and the solution of the corresponding homogeneous ODE system which is dependent on the initial state at the begin of the evolution at time $t=0$. The general solution of this system has the form

$$\begin{aligned} \Delta R(t) &= rn_S(t) \\ &= rn_S^1(0) \exp\left(-\left[d + \frac{r}{2} + w + \sqrt{\frac{r^2}{4} + w^2}\right]t\right) \\ &\quad + rn_S^2(0) \exp\left(-\left[d + \frac{r}{2} + w - \sqrt{\frac{r^2}{4} + w^2}\right]t\right). \end{aligned} \quad (2)$$

In this expression, the variable $\Delta R(t)$ represents the difference of the recombination rate at a given time from the steady state, the constants $n_S^i(0)$ contain the dependence from the initial conditions at time $t=0$.

The basic idea of the time domain measurement of spin-dependent recombination (TSR) experiment is to change the spin configuration within a KSM-pair ensemble by short (ns range) and intensive pulses (kW range) instead of long (ms range) and soft pulses (mW range) as it is done with conventional cw EDMR. The intensity has to be sufficiently strong such that the spin transition rate exceeds the dynamical recombination constants ($w \gg d, r$) during the pulse. In addition, the pulses have to be sufficiently short, such that the resonant steady state of the system is not reached at the end of the pulse. Under these conditions and the assumption that ($r \gg d$) as shown elsewhere,^{2,7,10} Eq. (2) becomes

$$\Delta R_{\text{res}}(t) = A(0)e^{-2wt} + B(0)e^{-r/2t}, \quad (3)$$

as long as the resonant radiation is applied. When the microwave is switched off at a time τ , the recombination rate change has reached its peak value $\Delta R(\tau)$ [see Fig. 2(a)] and relaxes according Eq. (2) as

$$\Delta R_{\text{rel}}(t) = C(\tau)e^{-r[t-\tau]} + D(\tau)e^{-d[t-\tau]}, \quad (4)$$

since the spontaneous spin flip probability is low ($w \ll d, r$) when the temperature is low enough. The constants $A(0)$, $B(0)$, $C(\tau)$, and $D(\tau)$ in Eqs. (3) and (4) depend on the initial conditions at the beginning ($t=0$) of the pulse and the end ($t=\tau$) of the pulse respectively. Figure 2(a) illustrates the fast recombination change during and shortly after the

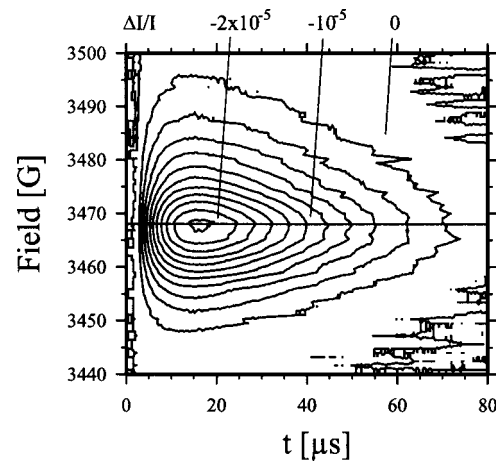


FIG. 3. Contour plot of the current quenching transients of undoped μc -Si:H taken at $T=5$ K. $\Delta I/I$ represents the relative current change. The horizontal line indicates a Landé g -factor of $g=2.0055$.

microwave pulse and Fig. 2(b) the slower rate relaxation on an extended time scale. For these calculations, we assumed that $\tau=160$ ns, $w=10^8$ s⁻¹ during the pulse and $w=0$ thereafter, $r=3 \times 10^6$ s⁻¹ and $d=2.5 \times 10^4$ s⁻¹.

The bottle neck of the experimental verification of the transient as illustrated in Fig. 2 is the time resolution of the current amplifier. The best state of the art current amplifiers can hardly exceed the MHz range at current charges in the pA range. This limitation leads to a signal deformation as illustrated by the dashed line of Fig. 2(b) where an amplifier time constant of 10 μ s has been assumed. In spite of this technological drawback, access to the reaction dynamics in the ns range is possible nevertheless. Since $C(\tau)$ and $D(\tau=t)$ in Eq. (4) are proportional to $\Delta R(\tau)$, the measurement of the amplitude of the relaxation signal for various pulse lengths does reveal the time behavior of the recombination transient during the pulse.

The TSR experiment is based on the fast transient measurement of recombination changes due to pulsed ESR. A Bruker E580 pulse ESR spectrometer (X-Band, 9.5 GHz) with ER4118 probe head and traveling wave tube amplifier was used for the generation of the short and intensive microwave pulses. The sample was cooled to $T=5$ K to minimize the spin flip probability w in Eq. (2) due to the spin-lattice relaxation time T_1 .

The model material that was used is nominally undoped microcrystalline silicon (μc -Si:H), deposited with electron cyclotron resonance chemical vapor deposition on a 1737 corning glass substrate. The sample had a thickness of 2.7 μ m and a dark conductivity of $\sigma_d=3.8 \times 10^{-4}$ Ω^{-1} cm⁻¹ at room temperature. As shown by Kanschat *et al.*,⁸ μc -Si:H provides strong signals of spin-dependent recombination through dangling bonds with a Landé factor of $g=2.0055$. Within the experimental resolution, the partners of the spin pair can not be resolved. Because of the critical time resolution, the sample resistance had to be kept as low as possible. Therefore, a meander shaped contact grid system was used. The signals were amplified by a Stanford Research SR570 high speed current amplifier and sampled by a Bruker SpecJet transient recorder. The photocharge carriers were generated by a 3 W cw-Ar-ion laser at a wavelength $\lambda=514$ nm.

For the suppression of current changes induced by the

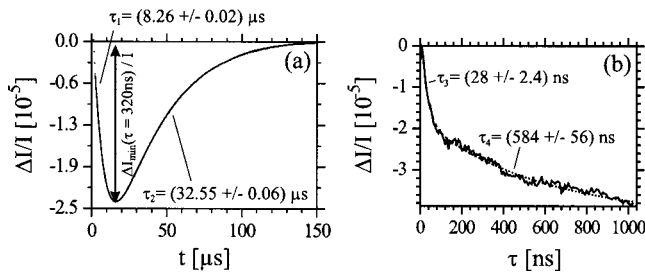


FIG. 4. (a) Current quenching transient after a 320 ns pulse and a double exponential fit (dashed line) of nominally undoped μc -Si:H at $T=5$ K and a field of $B=3468$ G. Note that the fit and the data are hardly distinguishable. The initial signal increase τ_1 is due to the amplifier time constant. (b) The transient amplitude $\Delta I_{\min}(\tau)/I$ versus the pulse length τ and a double exponential fit (dashed line).

intensive microwave radiation and by magnetoresistance, the resonant transients were obtained from the difference of the on-resonance transients and the average value of two off-resonance transients which were recorded at magnetic fields at equal distances above and below the resonant field. The center of the resonance was determined with a two-dimensional field sweep/time domain measurement. Figure 3 shows the raw data of such a sweep recorded at $T=5$ K and with 320 ns long pulses whose excitation width of about $\Delta B=1$ G determines the resolution of the illustrated graph. The slope of the quenching transient after the pulse is due to the amplifier time constant. After the signal has reached its maximum at $t=15 \mu s$, a slow signal relaxation takes place. The maximum signal amplitude is reached at a magnetic field of $B=3468$ G yielding a Landé factor of $g=2.0055$. This is in agreement with the predictions for dangling bond recombination in μc -Si:H by Kanschat *et al.*⁸ From the contour plot given in Fig. 3, one can also recognize the asymmetric field dependence of the transient which confirms the observations in Ref. 8, that a small resonant peak can be found at $g=1.998$ (which corresponds to $B=3480$ G), due to trap-dangling bond recombination.

Figure 4(a) shows the signal transient at $g=2.0055$. The double exponential fit of this graph reveals a time constant $\tau_1=(8.26 \pm 0.02) \mu s$ which is due to the amplifier time con-

stant and $\tau_2=(32.55 \pm 0.06) \mu s$ which yields according to Eq. (4) a value of $d=(3.1 \pm 0.1) 10^4 s^{-1}$. To determine the recombination probability r , the transient amplitude versus the pulse length was recorded as shown in Fig. 4(b). A double exponential fit reveals time constants of $\tau_3=(28 \pm 2.4) ns$ for the fast decay and $\tau_4=(584 \pm 56) ns$ for the slower decay. The constant τ_3 can be identified with the resonant spin flip rate $2w$. This was experimentally verified by changing the microwave power. The necessary assumptions of the model outlined are therefore met and the value for the recombination probability $r=(3.4 \pm 0.3) 10^6 s^{-1}$ can be calculated from τ_4 .

In conclusion, we show that the KSM model explains the dynamics of spin-dependent recombination. The use of very short and intensive resonant microwave pulses allows the direct measurement of charge carrier pair dissociation and recombination. This information reveals an understanding of the dynamics of distinct recombination processes and therefore gives access to new studies on electronically active defects in semiconductors. The feasibility of this characterization method (TSR) is demonstrated on the dangling-bond recombination process of microcrystalline silicon.

The authors thank M. Birkholz, E. Conrad, L. Elstner, S. Fiechter, K. Jacob, G. Keiler, D. Patzek, and B. Rabe for technical assistance as well as P. Kanschat and W. Fuhs for helpful discussions.

¹D. J. Lepine, Phys. Rev. B **6**, 436 (1972).

²D. Kaplan, I. Solomon, and N. F. Mott, J. Phys. (France) Lett. **39**, L51 (1978).

³M. Stutzmann, M. S. Brandt, and M. W. Bayerl, J. Non-Cryst. Solids **266**, 1 (2000).

⁴B. Stich, S. Greulich-Weber, and J.-M. Spaeth, J. Appl. Phys. **77**, 1546 (1995).

⁵J. H. Stasis, Appl. Phys. Lett. **68**, 1669 (1996).

⁶Z. Xiong and D. J. Miller, Appl. Phys. Lett. **63**, 352 (1993).

⁷T. Eickelkamp, S. Roth, and M. Mehring, Mol. Phys. **95**, 967 (1998).

⁸P. Kanschat, K. Lips, and W. Fuhs, J. Non-Cryst. Solids **266**, 524 (2000).

⁹F. C. Rong, G. J. Gerardi, W. R. Buchwald, E. H. Poindexter, M. T. Umlor, D. J. Keeble, and W. L. Warren, Appl. Phys. Lett. **60**, 610 (1991).

¹⁰I. Hiromitsu, Y. Kaimori, M. Kitano, and T. Ito, Phys. Rev. B **59**, 2151 (1999).